Submitted to Phys. Rev. B

Critical flux pinning and enhanced upper-critical-field in magnesium diboride films

Milind N. Kunchur,* Cheng Wu, and Boris I. Ivlev
Department of Physics and Astronomy
University of South Carolina, Columbia, SC 29208

Eun-Mi Choi, Kijoon H.P. Kim, W. N. Kang, and Sung-Ik Lee
National Creative Research Initiative Center for Superconductivity
and Department of Physics
Pohang University of Science and Technology
Pohang 790-784, Republic of Korea
(Dated: May 4, 2003)

We have conducted pulsed transport measurements on c-axis oriented magnesium diboride films over the entire relevant ranges of magnetic field $0 \lesssim H \lesssim H_{c2}$ (H_{c2} is the upper critical field) and current density $0 \lesssim j \lesssim j_d$ (j_d is the depairing current density). The intrinsic disorder of the films combined with the large coherence length and three-dimensionality (compared to cuprate superconductors) results in a large enhancement of the upper-critical-field H_{c2} and depinning current density j_c, raising the latter almost to j_d. The current-voltage response is highly non-linear at all fields, resulting from a combination of depinning and pair-breaking, and has no trace of an Ohmic free-flux-flow regime.

PACS numbers: 74.25.Sv, 74.25.Fy, 74.25.Bt

I. INTRODUCTION

Magnesium diboride (MgB_2) recently made an impact as a promising new superconductor with a surprisingly high critical temperature T_c for a simple binary compound. Besides the temperature T, the other principle parameters that define the operational space of a superconductor are magnetic field H and current density j. Superconductivity perishes above H_{c2} (T, j) and $j_d(T, H)$. For most practical applications it is not sufficient for the system to be merely in a superconducting state (presence of a finite order parameter amplitude) but for the system to be in a dissipationless state (constancy of order-parameter phase difference across sample length). Thus from a practical standpoint, the conventional critical current density j_c is limited by the depinning of vortices and their consequent motion. In the high-T_c cuprates, the large T_c is accompanied by high values[1] of j_d ($> 10^8$ A/cm^2). However the layered structure and small coherence length ξ lead to very weak vortex pinning. Thus between j_c and j_d, there can be a broad dissipative regime[2].

MgB_2 has an intermediate T_c and low values of j_d and H_{c2}. $j_d \sim 10^7$ A/cm^2 at low temperatures[3] and, in single crystals, $H_{c2} \sim 3$ T parallel to the c-axis[4]. In the films studied here, the intrinsic disorder makes two striking improvements. First of all H_{c2} is enhanced five-fold. Secondly, pinning is enhanced to the point of raising j_c almost to the value of j_d. These observations are consistent with the reduction of ξ with disorder. Finally MgB_2's normal-state resistivity ρ_n is lower than a typical cuprate superconductor (e.g., $Y_1Ba_2Cu_3O_7$) by two orders of magnitude. This increases the vortex viscosity by the same factor, so that even when the vortices are depinned, they flow at very low velocities causing insignificant dissipation until j_c becomes comparable to j_d. All these factors lead to an extremely steep non-linear current-voltage (IV) curve with a complete absence of an Ohmic regime characteristic of free flux flow[5].

II. EXPERIMENTAL DETAILS

The samples are 400 nm thick films of MgB_2 fabricated using a two-step method whose details are described elsewhere[6,7]. An amorphous boron film was deposited on a $(1\bar{1}02)$ Al_2O_3 substrate at room temperature by pulsed-laser ablation. The boron film was then put into a Nb tube with high-purity Mg metal (99.9%) and the Nb tube was then sealed using an arc furnace in an argon atmosphere. Finally, the heat treatment was carried out at 900° C for 30 min. in an evacuated quartz ampoule sealed under high vacuum. X-ray diffraction indicates a highly c-axis-oriented crystal structure normal to the substrate surface with no impurity phases. The films were photolithographically patterned down to narrow bridges. In this paper we show data on three bridges, labelled S, M, and L (for small, medium, and large) with lateral dimensions 2.8 x 33, 3.0 x 61, and 9.7 x 172 μm^2 respectively. The lateral dimensions are uncertain by $\pm 0.7 \mu$m and the thickness by ± 50 nm. Fig. 1(a) shows the sample geometry. The horizontal sections of the current leads contribute a small (~ 15 %) series resistance to the resistance of the actual bridge, which enters in measurements made at very small j. At high j in the mixed, the extra contribution is frozen out (because the current is spread out in these wider areas and ρ rises rapidly with j) and one observes mainly the resistance of the bridge.

The non-linear electrical transport measurements were made using a pulsed signal source with pulse durations ranging 0.1–4 μs and a duty cycle of about 1 ppm. At the other extreme, a conventional continuous DC method at a very low current ($I = 1.4 \mu$A) was employed for the resistive traces used to determine H_{c2}. Fig. 1(b) shows pulse waveforms under especially severe conditions ($j = 9.7$ MA/cm^2, $E = 83$ V/cm, and $p = jE = 803$ MW/cm^3). The resistance rises to (90% of) its final value in about 50 ns from the (10%) onset of I. From past experience with other films (e.g., $Y_1Ba_2Cu_3O_7$ on $LaAlO_3$) we found that micron-wide bridges typically have thermal resistances of order $R_{th} \sim$ 1–10 nK.cm^3/W at

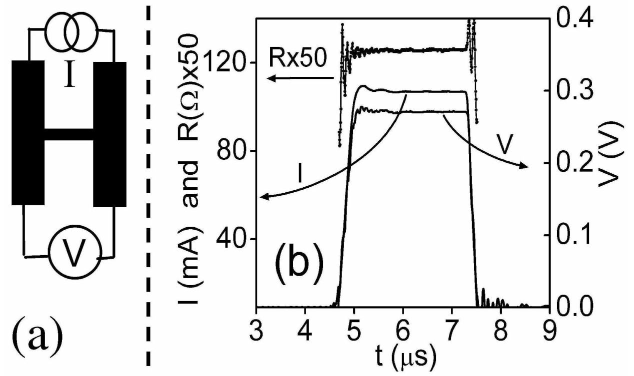

FIG. 1: *(a) Sample geometry used for resistance measurement. At low values of j the wide lead areas add a constant resistance of about 15% of the total value. At high j this contribution is frozen out. (b) Pulse waveforms under worst-case conditions (j = 9.7 MA/cm^2, E = 83 V/cm, and $p = jE$ = 803 MW/cm^3 on the plateaus). The resistance rises to (90% of) its final value in about 50 ns from the (10%) onset of I.*

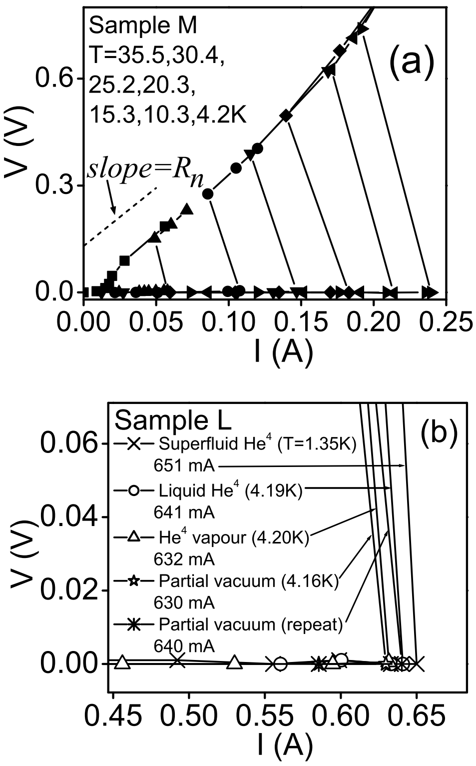

FIG. 2: *(a) IV curves in zero field for sample M at various indicated T. The resistance is driven to its normal-state value (R_n) by currents of pair-breaking magnitudes. (b) Similar curves for sample L in different thermal environments showing the paucity of sample heating.*

microsecond timescales[2,8,9]. For the present film-substrate combination, complete information about the thermal constants was not available to calculate R_{th} from first principles, but we expect a similar R_{th} of few nK.cm^3/W. To get some feel for the maximum R_{th}, consider the the IV curves shown in Fig. 2(a) for sample M in zero field. The different curves correspond to different values of T. Above some threshold the system is driven normal and it is shown elsewhere[3] that the rise in resistance is primarily due to pair breaking and not sample heating. Fig. 2(b) shows the bottom portions of such curves for sample L (the largest sample has the highest surface-to-volume ratio and hence represents the worst case thermal scenario). The different curves are in different thermal environments (superfluid liquid helium, normal liquid helium, helium vapour, and vacuum) to assess the role of sample heating[10]. Since there is no systematic shift in the threshold current with environment, one can conclude that heating is negligible (Incidentally if one pretends that the rise to the normal state is entirely due to sample heating and not pair-breaking, then setting $\rho_n j^2 R_{th} = T_c$ gives a grossly overestimated upperbound for R_{th} of 7 nK.cm^3/W.). In the present work, the power densities jE are much smaller than in the other (zero-field pair-breaking) work[3] and there is no question that sample heating is absolutely negligible. Note that we show the curves of Fig. 2 only for the purpose of addressing the question of heating and to explain the experimental techniques; the issue of pair-breaking is addressed elsewhere[3].

The magnetic field is applied normal to the film (parallel to the c axis) and the self field of the current is much lower than the applied fields used in this work. Further details of the measurement techniques have been published in a previous review article[2] and other recent papers[8,9].

III. RESULTS AND ANALYSIS

Fig. 3 shows the resistive transitions (at a low continuous current of $I = 1.4\mu$A) at different fixed magnetic fields for samples M and S (curves for sample L are similar). In the central region of the transition (emphasized in panel (b)) the shifts are relatively parallel, reducing the ambiguity of $H_{c2}(T)$ defined by the transition-midpoint criterion. Fig. 4 shows those $H_{c2}(T)$ values. $H_{c2}(T)$ has an unusual linear dependence that departs noticeably from the dashed line of the WHH (Werthamer-Helfand-Hohenberg) function[11]. This observation is consistent with a dirty two-gap superconductor as shown by Gurevich[12]. Panel (b) shows the $H_{c2}(T)$ for sample S defined at other criteria (see Fig. 3(b) above). Note that the linear dependence is preserved and the slopes (and hence inferred zero-T values of H_{c2}) do not change significantly with the choice of criteria. We infer a value of 17 ± 3 T for $H_{c2}(0)$, which is six times higher than the value of 3 T found in single crystals[4]. This can be understood in view of the much higher resistivity and hence shorter coherence length ξ: For a dirty superconductor effectively $\xi = \sqrt{\xi_0 l}$, where ξ_0 is the clean-limit value and l is the impurity scattering mean-free-path. On the other hand $\rho \propto l$ and $H_{c2} \propto 1/\xi^2$. Hence we expect $H_{c2} \propto \rho$. The normal resistivity of our film samples (14 $\mu\Omega$-cm) is about seven times higher than the value for their single crystals (2 $\mu\Omega$-cm). Note that this H_{c2} enhancement occurs naturally in the as-prepared films without any special effort to introduce pinning sites.

We now turn to the in-field IV curves to investigate the nature of flux motion. In a system with weak flux pinning, the resistance goes through alternate regimes of Ohmic (homogeneously linear dependence of V on I) and non-Ohmic behavior. At very low driving forces (low j) there can be

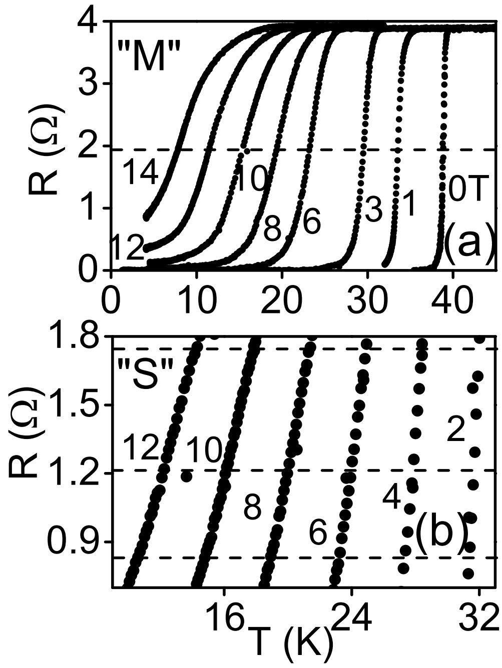

FIG. 3: *Resistive transitions of two MgB_2 bridges at indicated flux densities. I=1.4 μA. (a) Sample M; midpoint T_c's lie on the dashed line through $R = R_n/2 = 1.95\Omega$. (b) Similar set for sample S. Dashed lines run through $R = R_n/2 = 1.22\Omega$, and also through the lower and higher resistive criteria $R = 0.84\Omega$ and $R = 1.76\Omega$.*

observable resistance due to thermally activated flux flow (TAFF) or flux creep. Then one encounters a non-linear response as current driven depinning sets in; in effect the number of mobile vortices is rising. This is incipient flux flow. At sufficiently larger j, the vortex motion is effectively free from the influence of pinning and the response becomes Ohmic again. We previously introduced the term *free flux flow* (FFF) for this linear regime[5]. Here the dissipation and resistivity should correspond to the canonical $\rho_f \sim \rho_n B/H_{c2}$ Bardeen-Stephen expression (somtimes large departures can occur for exceptional situations such as superclean systems and narrow vortex cores where the internal energy-level spacing exceeds their widths). As one goes beyond FFF, nonlinearity can set in because of heating of the electron gas[13] or changes in the electron distribution function[14]. Finally at yet higher currents, pair-breaking destroys superconductivity and drives the system normal. Here the resistance again ceases to change with current, being characteristic of the normal state, and so the response becomes Ohmic one more time. Our previous review article discusses some of these stages of dissipation. In $Y_1Ba_2Cu_3O_7$, the depinning critical current is sufficiently weak compared to the pair-breaking value that all of these fascinating regimes can be observed.

In MgB_2 the situation is very different. Fig. 5(a) shows the R(I) curves of the present MgB_2 samples. After the onset of dissipation, the resistance quickly rises to the full normal-state value. It should be noted that the plateaus do not correspond to FFF but to the normal state. Accordingly the resistance value changes very little with the applied B, especially for the curves at lower fields[15]. It is interesting

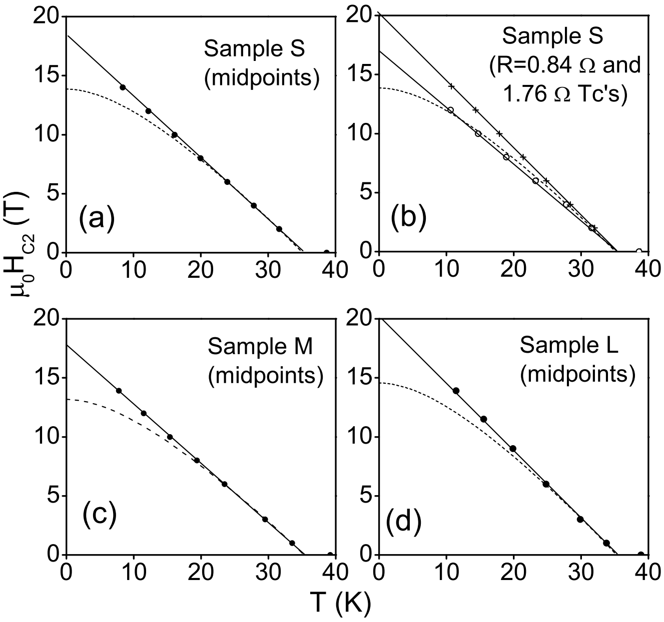

FIG. 4: *H_{c2} versus B for three samples. The solid straight lines are linear fits to the data. The dashed lines correspond to the WHH function.*

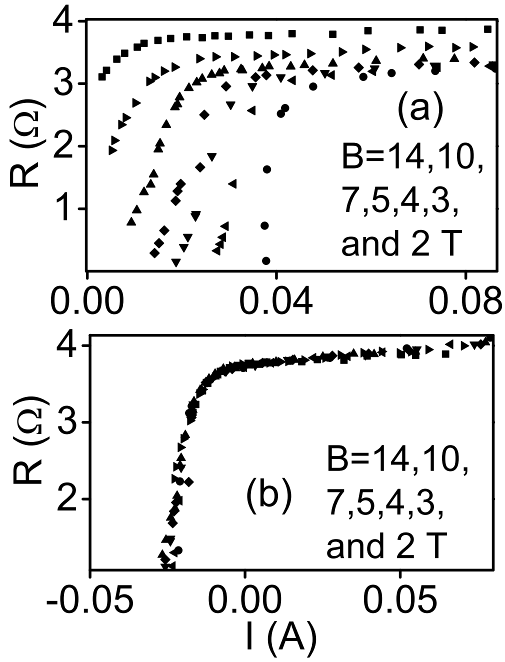

FIG. 5: *Resistance versus current curves for sample M. Flux densities are indicated from left to right. The sample was emersed in superfluid helium and $T = 1.5K$ for all data. (a) Raw data. (b) Same data linearly shifted so as to collapse onto a single common behavior.*

to note that the overall shapes of the curves are almost independent of field. When the curves of the previous panels are shifted vertically and horizontally by constant amounts they can be made to overlap as shown in Fig. 5(b). Fig. 6 shows the raw and shifted curves for the other two samples.

These steep IV characteristics bear similarity to niobium alloys but are markedly different from the cuprates. The

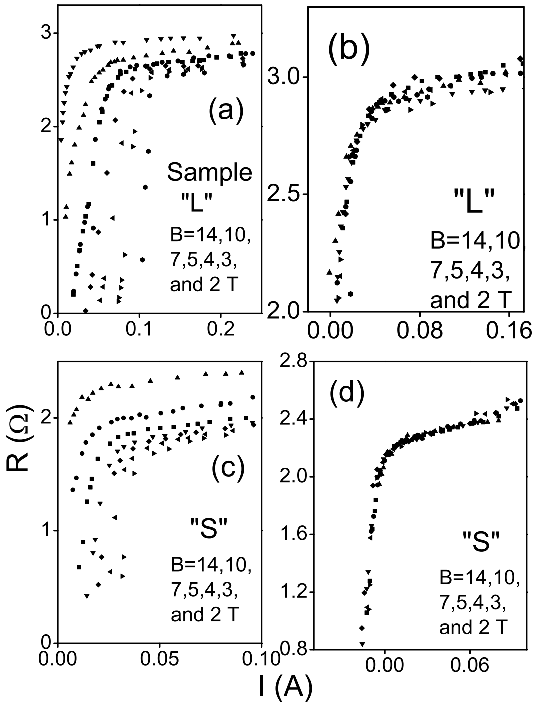

FIG. 6: *Resistance versus current curves for samples S and L. Flux densities are indicated from left to right. The sample was emersed in superfluid helium and $T = 1.5K$ for all data. Panels in the left column show raw data and panels in the right column show linearly shifted data.*

latter can be understood in terms of the lower temperature scale (T_c less than half that of $Y_1Ba_2Cu_3O_7$) and much greater pinning (more isotropic and 3-D like; ten times larger vortex cross section: $\xi = 5$ instead of 1.6 nm). Hence thermal activation and current driven depinning are deferred until j becomes almost comparable to j_d, causing the response to become steeply non-linear rising from very little dissipation to the full normal state within a rather narrow range of currents. The scaling in Figs. 6 and 5 seems to suggest that the rise in resistance stems as much from pair-breaking by the current and field, as due to current driven depinning. All this may make for a brief and relatively uninteresting IV curve from a fundamental standpoint, however it makes MgB_2 films attractive for practical applications. Even though j_d in this material is about an order of magnitude lower than many cuprates[1,3] the flux dissipation sets in so much later that the practically useable current densities are higher than might be inferred from the j_d of the material.

IV. CONCLUSIONS

We have investigated the low-temperature ($T \ll T_c$) in-field transport behavior of MgB_2 and present the first measurement of the full dissipation curves (i.e., $0 \le j \lesssim j_d$ and $0 \le R_{T=0} \lesssim R_n$) for this system. MgB_2 films made by the two-step laser-ablation process have intrinsically strong pinning, leading to ususually steep IV curves. The onset of dissipation is within an order of magnitude of the pairbreaking current, even at flux densities of a few Teslas, and the resistance quickly rises to the full normal-state value as the current is increased beyond j_c. The same disorder that enhances pinning, also enhances H_{c2} and qualitatively changes its temperature dependence because of the two-band nature of the superconductivity in this material. As explained by the theory of Gurevich, $H_{c2}(0)$ extrapolates to a higher value than dictated by the WHH type of behavior, and the dH_{c2}/dt slope is relatively constant. Our measurements of H_{c2} confirm this predicted unusual dependence. These qualities make such MgB_2 films very promising for applications.

V. ACKNOWLEDGEMENTS

The authors acknowledge useful discussions with J. M. Knight and A. Gurevich. This work was supported by the U. S. Department of Energy through grant number DE-FG02-99ER45763 and by the Ministry of Science and Technology of Korea through the Creative Research Initiative Program.

---

* URL: `http://www.physics.sc.edu/kunchur`; Electronic address: `kunchur@sc.edu`

1 M. N. Kunchur, D. K. Christen, C. E. Klabunde, and J. M. Phillips, Phys. Rev. Lett. **72**, 752 (1994).
2 M. N. Kunchur, Mod. Phys. Lett. B. **9**, 399 (1995).
3 M. N. Kunchur et al., submitted to Phys. Phys. Lett.
4 Phys. Rev. B 65, 180505(R) (2002); and O. F. de Lima et al., Phys. Rev. Lett. **87**, 47002 (2001).
5 M. N. Kunchur, D. K. Christen, and J. M. Phillips, Phys. Rev. Lett. **70**, 998 (1993).
6 W. N. Kang et al., Science 292, 1521 (2001).
7 W. N. Kang et al., Physica C **385**, 24 (2003).
8 M. N. Kunchur, Phys. Rev. Lett. **89**, 137005 (2002).
9 M. N. Kunchur, B. I. Ivlev, D. K. Christen, J. M. Phillips, Phys. Rev. Lett. 84, 5204 (2000).
10 O. M. Stoll, S. Kaiser, R. P. Huebener, and M. Naito, Phys. Rev. Lett. **81**, 2994 (2001).
11 N. R. Werthamer, E. Helfand, and P. C. Hohenberg, Phys. Rev. **147**, 295 (1966).
12 A. Gurevich, preprint.
13 M. N. Kunchur, Phys. Rev. Lett. **89**, 137005 (2002).
14 A. I. Larkin and Yu. N. Ovchinnikov, Zh. Eksp. Teor. Fiz. **68**, 1915 (1975) [Sov. Phys. JETP **41**, 960 (1976)].
15 The slight shift in plateau resistance at the highest fields can be understood in terms of spreading of resistance outside the bridge area and into the current-lead areas as explained in the experimental section. Fields approaching H_{c2} start driving the whole film normal at relatively low currents so that the resistance of the wider current-lead areas is not frozen out. This causes the normal-state plateau to rise slightly at the highest fields.